Implication of $R_{D^{(*)}}$ anomalies on semileptonic decays of Σ_b and Ω_b baryons

N. Rajeev[*] and Rupak Dutta[†]
National Institute of Technology Silchar, Silchar 788010, India

Suman Kumbhakar[‡]
Indian Institute of Technology Bombay, Mumbai 400076, India

(Received 5 June 2019; published 19 August 2019)

The flavor changing decays of heavy bottom quarks to the corresponding lighter quarks (u, c, and s) in various B-meson decays via charged current and neutral current semileptonic transitions have emerged as promising candidates to explore physics beyond the standard model. Experimentally the lepton flavor universality violation in $b \to (c, u)l\nu$ and $b \to sl^+l^-$ transitions have been reported to a higher precision. The measurements of the lepton flavor violating ratios such as $R_{D^{(*)}}$, $R_{J/\Psi}$, and $R_{K^{(*)}}$ are observed to deviate from the standard model expectations at the level of 1.4σ, 2.5σ, 1.5σ, 2.4σ, and 2.2σ respectively. Motivated by these anomalies, we investigate the lepton flavor universality violation in $\Sigma_b \to \Sigma_c l\nu$ and $\Omega_b \to \Omega_c l\nu$ decays. We follow a model independent effective field theory formalism and study the implications of $R_{D^{(*)}}$ anomalies on $\Sigma_b \to \Sigma_c \tau\nu$ and $\Omega_b \to \Omega_c \tau\nu$ decay modes. We give predictions of various physical observables such as the ratio of branching ratios, total differential decay rate, forward-backward asymmetry, lepton side polarization fraction, and convexity parameter within the standard model and within various new physics scenarios.

DOI: 10.1103/PhysRevD.100.035015

I. INTRODUCTION

Although, the present-day experimental results in B factory experiments are dominated by the meson decays over the baryon decays, the theoretical exploration of the semileptonic decays of baryons have a longer history as compared to the mesons. The system of particles which are classified under mesons and baryons are mainly distinguished by their quark structure. In the early 1960s the concept of diquarks emerged out of some critical phenomenological ideas and have lead to the diverse coherent thoughts about the baryon decay characteristics. Soon after in Refs. [1,2] the concept of a diquark was literally introduced in order to describe a baryon as a composite state of two particles called a quark and a diquark. The heavy quark symmetry assumes baryons as a bound state of (Qqq) where Q is the heavy quark surrounded by the lighter quarks q. This idea of a quark-diquark picture of a baryon has successfully managed to predict various properties including their compositions and the decay probabilities. During the weak decays of baryons, only the heavier quark will be knocked out of a baryon and take part in the decay process by changing its flavor whereas the lighter diquark pair will act as a spectator [3]. This is because when we carefully monitor this process, the quantum numbers (color index, helicities, momentum) are conserved for the lighter diquark system. Hence, this baryon three-body problem is reduced to a usual meson two-body problem (see Fig. 1). Therefore, at the scale of quark level transitions, the treatment of semileptonic decays of baryons are considered to be very much analogous to that of mesons.

The study of semileptonic B meson decays is of great interest due to the long-standing anomalies that are present in various B meson decays mediated via $b \to cl\nu$ and

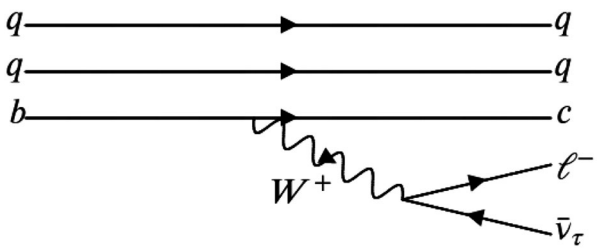

FIG. 1. Tree level Feynman diagram representing the transitions of $\Sigma_b^-(ddb) \to \Sigma_c^0(ddc)l^-\bar{\nu}_l$ and $\Omega_b^-(ssb) \to \Omega_c^0(ssc)l^-\bar{\nu}_l$.

[*]rajeev@rs.phy.student.nits.ac.in
[†]rupak@phy.nits.ac.in
[‡]suman@phy.iitb.ac.in

$b \to s l^+ l^-$ quark level transitions. The most well-grounded measurements which substantiate these anomalies are the ratio of branching ratios R_D and R_{D^*} defined as

$$R_D = \frac{\mathcal{B}(B \to D\tau\nu)}{\mathcal{B}(B \to D\{e/\mu\}\nu)}, \qquad R_{D^*} = \frac{\mathcal{B}(B \to D^*\tau\nu)}{\mathcal{B}(B \to D^*\{e/\mu\}\nu)}. \tag{1}$$

The precise standard model (SM) predictions of R_D and R_{D^*} based on the recent lattice calculations have been carried out by various groups and interestingly every prediction is in good agreement with each other. The FNAL/MILC Collaboration predicts the value of R_D to be 0.299 ± 0.011 [4]. Similarly, in Ref. [5] it is predicted to be 0.300 ± 0.008. By combining these two calculations the FLAG working group [6] has come up with a value of $R_D = 0.300 \pm 0.008$. The authors in Ref. [7] suggest a more accurate value of $R_D = 0.299 \pm 0.003$ by combing the two lattice calculations by obtaining the experimental form factors of $B \to Dl\nu$ from *BABAR* and Belle. In fact various similar calculations of R_D can also be found in Refs. [8,9]. Regarding the R_{D^*} SM predictions, at present we have quite a large number of predictions in which every prediction manifests a minimal variation. In Ref. [10] the authors predicted the value to be $R_{D^*} = 0.252 \pm 0.003$. More recent calculations of $R_{D^*} = 0.257 \pm 0.003$ [8], 0.257 ± 0.005 [9], and 0.260 ± 0.008 [11] obtained from the new form factor inputs by fitting the unfolded spectrum from Belle with the BGL parametrization [12] are in good agreement with each other as well as with the previous prediction. One can expect an even more precise prediction of R_{D^*} once the full lattice QCD calculations are available. On the other hand, we have several measurements of R_D and R_{D^*} from various experiments such as *BABAR*, Belle, and LHCb. The Heavy Flavor Averaging Group (HFLAV) determined the combined deviation in $R_{D^{(*)}}$ with respect to the SM. Recent measurements from Belle in 2019 have a significant impact on the average values of $R_{D^{(*)}}$. At present the combined deviation in $R_{D^{(*)}}$ is reported to be 3.08σ from the SM expectations. The average values of R_D and R_{D^*} reported by HFLAV are displayed in Table I.

The clear disagreements between the SM predictions and the experimental measurements strongly indicate possible new physics. Several new physics scenarios are being investigated within model dependent and model independent frameworks [23–42]. Similarly, implications of $R_{D^{(*)}}$ anomalies on similar decay modes have been studied as well. The details can be found in Refs. [43–53].

Apart from R_D and R_{D^*} measurements, the LHCb has also measured the ratio of branching ratio $R_{J/\Psi} = \mathcal{B}(B_c \to J/\Psi\tau\nu)/\mathcal{B}(B_c \to J/\Psi l\nu)$ to be $0.71 \pm 0.17 \pm 0.18$ [54] which stands around 1.3σ away from the SM value of [0.20, 0.39] [55]. As this error is relatively large, we do not consider $R_{J/\Psi}$ in our new physics (NP) analysis.

In the SM, the Σ_b and Ω_b semileptonic decays have been studied by several authors using the $\Sigma_b \to \Sigma_c$ and $\Omega_b \to \Omega_c$ transition form factors obtained in the spectator-quark model, the relativistic quark model, the Bethe-Salpeter approach, relativistic three-quark model, and the light-front quark model [56–67]. The total decay rate Γ (in units of 10^{10} s^{-1}) predicted within these models ranges from 1.44 to 2.23 for $\Sigma_b \to \Sigma_c e\nu$ and 1.29 to 1.87 for $\Omega_b \to \Omega_c e\nu$. These variations in the prediction of Γ may be due to the complexity in understanding the baryon structures and also due to the lack of precise predictions of various form factors. Nevertheless, we explore the NP effects on various observables pertaining to $\Sigma_b \to \Sigma_c \tau\nu$ and $\Omega_b \to \Omega_c \tau\nu$ decays within the model independent effective field theory formalism. It is indeed essential to study these decay modes both theoretically and experimentally to test the lepton flavor universality violation (LFUV).

We hope that there are good chances of studying these decays experimentally as the present-day LHC own plenty of data on heavy baryons. It may be difficult to measure the $\Sigma_b \to \Sigma_c l\nu$ branching ratio as Σ_b can decay strongly and hence their weak branching ratios will be very small [68]. However, measurement of an $\Omega_b \to \Omega_c l\nu$ branching ratio will be feasible because Ω_b decays predominantly weakly and has a significantly large semileptonic branching ratio. One can estimate the branching ratios for $\Omega_b \to \Omega_c l\nu$ decays which are found to be of the order of 10^{-2} for electron and 10^{-3} for tau final states. Hence it is worth studying these decay modes as they can give complimentary information regarding possible new physics [56,60,67].

Investigating the implications of $R_{D^{(*)}}$ on $\Sigma_b \to \Sigma_c \tau\nu$ and $\Omega_b \to \Omega_c \tau\nu$ decays will draw more interesting results. For this study, we have considered the form factors obtained in the relativistic quark model [56]. We give predictions of various observables within the SM and within various NP scenarios. The results pertaining to the lepton side forward-backward asymmetry and the convexity parameter are predicted in the SM for the first time in both the decay modes. Also, the new physics studies on these particular decay modes have not been explored until today.

The paper is organized as follows: In Sec. II, we briefly review the effective Lagrangian in the presence of the new

TABLE I. Recent SM predictions and world averages of R_D and R_{D^*}.

Observables	SM predictions	World averages	Deviation
$R_D = \mathcal{B}(B \to D\tau\nu)/\mathcal{B}(B \to Dl\nu)$	0.299 ± 0.003 [4–7]	$0.340 \pm 0.027 \pm 0.013$ [13–16]	1.4σ
$R_{D^*} = \mathcal{B}(B \to D^*\tau\nu)/\mathcal{B}(B \to D^*l\nu)$	0.258 ± 0.005 [8–11]	$0.295 \pm 0.011 \pm 0.008$ [13–22]	2.5σ

physics couplings. Next we discuss the helicity formalism for $\Sigma_b \to \Sigma_c$ and $\Omega_b \to \Omega_c$ transitions and write down the respective vector, axial-vector, scalar, and pseudoscalar helicity amplitudes. We also write down the formulas to calculate the total differential decay rate and various q^2 dependant observables. In Sec. III, we discuss the numerical results with all necessary input parameters. The numerical results are reported within the SM and within various NP scenarios. Finally, we conclude with a brief summary of our results in Sec. IV.

II. METHODOLOGY

Effective field theory formalism is a natural way to separate the effects coming from different scales involved in weak decays. The most relevant effective Hamiltonian for $b \to c l\nu$ transition decays represented at the scale of a bottom quark, containing both the SM and the possible NP operators, is defined as [69,70]

$$\mathcal{H}_{\rm eff} = \frac{4G_F}{\sqrt{2}} V_{cb}[(1+V_L)\mathcal{O}_{V_L} + V_R\mathcal{O}_{V_R} + S_L\mathcal{O}_{S_L} + S_R\mathcal{O}_{S_R} + T\mathcal{O}_T] + \text{H.c.}, \quad (2)$$

where G_F is the Fermi coupling constant, V_{cb} is the CKM matrix element, and V_L, V_R, S_L, S_R, and T are the Wilson coefficients (WCs) corresponding to the vector, scalar, and tensor NP operators. The Fermionic operators $\mathcal{O}_{V_L}$, $\mathcal{O}_{V_R}$, $\mathcal{O}_{S_L}$, $\mathcal{O}_{S_R}$, and $\mathcal{O}_T$ are defined as

$$\mathcal{O}_{V_L} = (\bar{c}\gamma^\mu b_L)(\bar{l}_L\gamma_\mu\nu_{lL}), \qquad \mathcal{O}_{V_R} = (\bar{c}\gamma_\mu b_R)(\bar{l}_L\gamma_\mu\nu_{lL}) \quad (3)$$

$$\mathcal{O}_{S_L} = (\bar{c}b_L)(\bar{l}_R\nu_{lL}), \qquad \mathcal{O}_{S_R} = (\bar{c}b_R)(\bar{l}_R\nu_{lL}) \quad (4)$$

$$\mathcal{O}_T = (\bar{c}\sigma^{\mu\nu}b_L)(\bar{l}_R\sigma_{\mu\nu}\nu_{lL}). \quad (5)$$

Here, we assume the neutrino to be always left chiral and all the WCs to be real. We rewrite the effective Lagrangian by considering NP contributions only from the vector and scalar type interactions as [71]

$$\mathcal{L}_{\rm eff} = -\frac{G_F}{\sqrt{2}} V_{cb}\{G_V\bar{l}\gamma_\mu(1-\gamma_5)\nu_l\bar{c}\gamma^\mu b - G_A\bar{l}\gamma_\mu(1-\gamma_5) \times \nu_l\bar{c}\gamma^\mu\gamma_5 b + G_S\bar{l}\gamma_\mu(1-\gamma_5)\nu_l\bar{c}b - G_P\bar{l}\gamma_\mu(1-\gamma_5)\nu_l\bar{c}\gamma_5 b\} + \text{H.c.}, \quad (6)$$

where

$$G_V = 1+V_L+V_R, \qquad G_A = 1+V_L-V_R,$$
$$G_S = S_L+S_R, \qquad G_P = S_L-S_R. \quad (7)$$

Within the SM, $V_{L,R} = S_{L,R} = 0$.

Using the effective Lagrangian of Eq. (6), the three body differential decay distribution for the $B_1 \to B_2 l\nu$ decays can be written as

$$\frac{d^2\Gamma}{dq^2 d\cos\theta} = \frac{G_F^2|V_{cb}|^2|\vec{P}_{B_2}|}{2^9\pi^3 m_{B_1}^2}\left(1-\frac{m_l^2}{q^2}\right)L_{\mu\nu}H^{\mu\nu}, \quad (8)$$

where $L_{\mu\nu}$ and $H^{\mu\nu}$ are the leptonic and hadronic current tensors. Here $|\vec{P}_{B_2}| = \sqrt{\lambda(m_{B_1}^2, m_{B_2}^2, q^2)}/2m_{B_1}$ with $\lambda(a,b,c) = a^2+b^2+c^2-2(ab+bc+ca)$ represents the three momentum vector of the outgoing baryon. One can use the helicity techniques for the covariant contraction of $L_{\mu\nu}$ and $H^{\mu\nu}$, details of which can be found in Refs. [72,73]. We follow Ref. [71] and write the expression for differential decay distribution for $B_1 \to B_2 l\nu$ decays in terms of the helicity amplitudes as follows:

$$\frac{d^2\Gamma}{dq^2 d\cos\theta} = N\left(1-\frac{m_l^2}{q^2}\right)^2\left[\mathcal{A}_1 + \frac{m_l^2}{q^2}\mathcal{A}_2 + 2\mathcal{A}_3 + \frac{4m_l}{\sqrt{q^2}}\mathcal{A}_4\right] \quad (9)$$

where θ is the angle between the $\vec{P}_{B_2}$ and lepton three momentum vector in the $l-\nu$ rest frame and

$$N = \frac{G_F^2|V_{cb}|^2 q^2|\vec{P}_{B_2}|}{512\pi^3 m_{B_1}^2}\left(1-\frac{m_l^2}{q^2}\right)^2,$$

$$\mathcal{A}_1 = 2\sin^2\theta\left(H_{\frac{1}{2}0}^2 + H_{-\frac{1}{2}0}^2\right) + (1-\cos\theta)^2 H_{\frac{1}{2}1}^2 + (1+\cos\theta)^2 H_{-\frac{1}{2}-1}^2,$$

$$\mathcal{A}_2 = 2\cos^2\theta\left(H_{\frac{1}{2}0}^2 + H_{-\frac{1}{2}0}^2\right) + \sin^2\theta\left(H_{\frac{1}{2}1}^2 + H_{-\frac{1}{2}-1}^2\right) + 2\left(H_{\frac{1}{2}t}^2 + H_{-\frac{1}{2}t}^2\right) - 4\cos\theta\left(H_{\frac{1}{2}t}H_{\frac{1}{2}0} + H_{-\frac{1}{2}t}H_{-\frac{1}{2}0}\right),$$

$$\mathcal{A}_3 = \left(H_{\frac{1}{2}0}^{SP}\right)^2 + \left(H_{-\frac{1}{2}0}^{SP}\right)^2,$$

$$\mathcal{A}_4 = -\cos\theta\left(H_{\frac{1}{2}0}H_{\frac{1}{2}0}^{SP} + H_{-\frac{1}{2}0}H_{-\frac{1}{2}0}^{SP}\right) + \left(H_{\frac{1}{2}t}H_{\frac{1}{2}0}^{SP} + H_{-\frac{1}{2}t}H_{-\frac{1}{2}0}^{SP}\right). \quad (10)$$

A. Form factors and helicity amplitudes

The hadronic matrix elements of vector and axial vector currents between two spin half baryons are parametrized in terms of the following form factors:

$$M_\mu^V = \langle B_2,\lambda_2|\bar{c}\gamma_\mu b|B_1,\lambda_1\rangle = \bar{u}_2(p_2,\lambda_2)[f_1(q^2)\gamma_\mu + if_2(q^2)\sigma_{\mu\nu}q^\nu + f_3(q^2)q_\mu]u_1(p_1,\lambda_1),$$
$$M_\mu^A = \langle B_2,\lambda_2|\bar{c}\gamma_\mu\gamma_5 b|B_1,\lambda_1\rangle = \bar{u}_2(p_2,\lambda_2)[g_1(q^2)\gamma_\mu + ig_2(q^2)\sigma_{\mu\nu}q^\nu + g_3(q^2)q_\mu]\gamma_5 u_1(p_1,\lambda_1), \quad (11)$$

where $q^\mu = (p_1-p_2)^\mu$ is the four momentum transfer, λ_1 and λ_2 are the respective helicities of the parent and

daughter baryons, and $\sigma_{\mu\nu} = \frac{i}{2}[\gamma_\mu\gamma_\nu]$. Here, B_1 represents the bottomed baryon Σ_b or Ω_b and B_2 represents the charmed baryon Σ_c or Ω_c. In the heavy quark limit, these matrix elements can be parametrized in terms of four velocities v^μ and v'^μ as follows:

$$\begin{aligned}
M_\mu^V &= \langle B_2,\lambda_2|\bar{c}\gamma_\mu b|B_1,\lambda_1\rangle = \bar{u}_2(p_2,\lambda_2)[F_1(w)\gamma_\mu + F_2(w)v_\mu \\
&\quad + F_3(w)v'_\mu]u_1(p_1,\lambda_1), \\
M_\mu^A &= \langle B_2,\lambda_2|\bar{c}\gamma_\mu\gamma_5 b|B_1,\lambda_1\rangle = \bar{u}_2(p_2,\lambda_2)[G_1(w)\gamma_\mu \\
&\quad + G_2(w)v_\mu + G_3(w)v'^\mu]\gamma_5 u_1(p_1,\lambda_1),
\end{aligned} \tag{12}$$

where $w = v.v' = (m_{B_1}^2 + m_{B_2}^2 - q^2)/2m_{B_1}m_{B_2}$ and m_{B_1} and m_{B_2} are the masses of the B_1 and B_2 baryons, respectively. One can compute the hadronic form factors for scalar and pseudoscalar currents by using the equation of motion. Those matrix elements are

$$\begin{aligned}
&\langle B_2,\lambda_2|\bar{c}b|B_1,\lambda_1\rangle \\
&= \bar{u}_2(p_2,\lambda_2)\left[f_1(q^2)\frac{q}{m_b - m_c} + f_3(q^2)\frac{q^2}{m_b - m_c}\right] \\
&\quad \times u_1(p_1,\lambda_1), \\
&\langle B_2,\lambda_2|\bar{c}\gamma_5 b|B_1,\lambda_1\rangle \\
&= \bar{u}_2(p_2,\lambda_2)\left[-g_1(q^2)\frac{q}{m_b + m_c} - g_3(q^2)\frac{q^2}{m_b + m_c}\right] \\
&\quad \times \gamma_5 u_1(p_1,\lambda_1),
\end{aligned} \tag{13}$$

where m_b and m_c are the respective masses of b and c quarks calculated at the renormalization scale $\mu = m_b$. These two sets of form factors are related through the following relations as given below and the q^2 behavior of form factors $f's$ and $g's$ are displayed in Fig. 2.

$$\begin{aligned}
f_1(q^2) &= F_1(q^2) + (m_{B_1} + m_{B_2})\left[\frac{F_2(q^2)}{2m_{B_1}} + \frac{F_3(q^2)}{2m_{B_2}}\right], \\
f_2(q^2) &= \frac{F_2(q^2)}{2m_{B_1}} + \frac{F_3(q^2)}{2m_{B_2}}, \\
f_3(q^2) &= \frac{F_2(q^2)}{2m_{B_1}} - \frac{F_3(q^2)}{2m_{B_2}}, \\
g_1(q^2) &= G_1(q^2) - (m_{B_1} - m_{B_2})\left[\frac{G_2(q^2)}{2m_{B_1}} + \frac{G_3(q^2)}{2m_{B_2}}\right], \\
g_2(q^2) &= \frac{G_2(q^2)}{2m_{B_1}} + \frac{G_3(q^2)}{2m_{B_2}}, \\
g_3(q^2) &= \frac{G_2(q^2)}{2m_{B_1}} - \frac{G_3(q^2)}{2m_{B_2}}.
\end{aligned} \tag{14}$$

In the heavy quark limit, the form factors can be expressed in terms of the Isgur-Wise function $\zeta_1(w)$ as follows [56]:

$$\begin{aligned}
F_1(w) &= G_1(w) = -\frac{1}{3}\zeta_1(w), \\
F_2(w) &= F_3(w) = \frac{2}{3}\frac{2}{w+1}\zeta_1(w), \\
G_2(w) &= G_3(w) = 0.
\end{aligned} \tag{15}$$

The explicit expression for $\zeta_1(w)$ is found to be

$$\zeta_1(w) = \lim_{m_Q\to\infty}\int\frac{d^3p}{(2\pi)^3}\Psi_{B_2}\left(\mathbf{p} + 2\boldsymbol{\epsilon}_d(p)\sqrt{\frac{w-1}{w+1}}\mathbf{e}_\Delta\right)\Psi_{B_1}(\mathbf{p}) \tag{16}$$

where $\mathbf{e}_\Delta = \Delta/\sqrt{\Delta^2}$, a unit vector in the direction of $\Delta = M_{B_2}\mathbf{v} - M_{B_1}\mathbf{v}$, and B_1 and B_2 are the parent and daughter baryon respectively. We refer to Ref. [56] for all the omitted details.

The relation between the hadronic matrix elements and the helicity amplitudes are defined as [72,74,75]

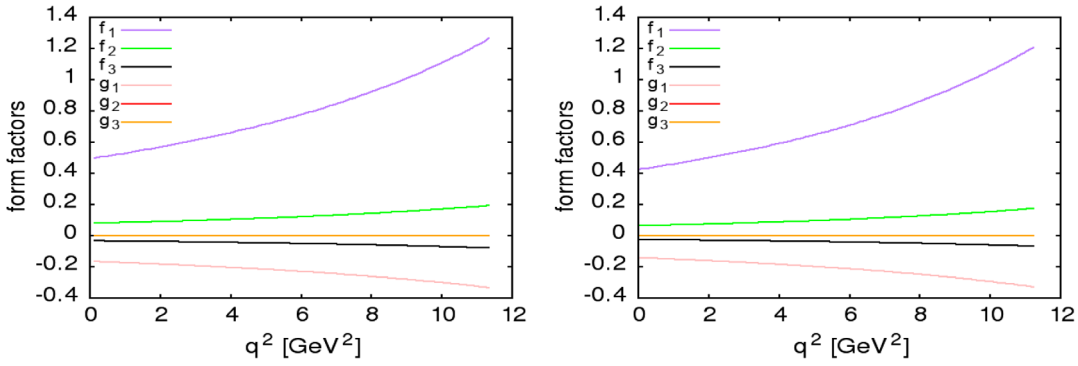

FIG. 2. $\Sigma_b \to \Sigma_c$ (left) and $\Omega_b \to \Omega_c$ (right) transition form factors as a function of q^2.

$$H^{V/A}_{\lambda_2\lambda_W} = M^{V/A}_{\mu}(\lambda_2)\epsilon^{\dagger\mu}(\lambda_W), \tag{17}$$

where λ_2 and λ_W are the respective helicities of the daughter baryon and the off-shell W boson. In the rest frame of parent baryon B_1, the helicity amplitudes can be written as [76,77]

$$\begin{aligned}
H^V_{\frac{1}{2}0} &= G_V\frac{\sqrt{Q_-}}{\sqrt{q^2}}[m_+f_1(q^2) - q^2f_2(q^2)],\\
H^A_{\frac{1}{2}0} &= G_A\frac{\sqrt{Q_+}}{\sqrt{q^2}}[m_-g_1(q^2) + q^2g_2(q^2)],\\
H^V_{\frac{1}{2}1} &= G_V\sqrt{2Q_-}[-f_1(q^2) + m_+f_2(q^2)],\\
H^A_{\frac{1}{2}1} &= G_A\sqrt{2Q_+}[-g_1(q^2) - m_-g_2(q^2)],\\
H^V_{\frac{1}{2}t} &= G_V\frac{\sqrt{Q_+}}{\sqrt{q^2}}[m_-f_1(q^2) + q^2f_3(q^2)],\\
H^A_{\frac{1}{2}t} &= G_A\frac{\sqrt{Q_-}}{\sqrt{q^2}}[m_+g_1(q^2) - q^2g_3(q^2)],
\end{aligned} \tag{18}$$

where $Q_\pm = (m_{B_1} \pm m_{B_2})^2 - q^2$ and $m_\pm = (m_{B_1} \pm m_{B_2})$. For the helicity flipped components, these amplitudes turn out to be $H^V_{-\lambda_2-\lambda_W} = H^V_{\lambda_2\lambda_W}$ and $H^A_{-\lambda_2-\lambda_W} = -H^A_{\lambda_2\lambda_W}$. Hence, the total left-handed helicity amplitude is

$$H_{\lambda_2\lambda_W} = H^V_{\lambda_2\lambda_W} - H^A_{\lambda_2\lambda_W}. \tag{19}$$

The scalar/pseudoscalar helicity amplitudes are defined as

$$\begin{aligned}
H^{SP}_{\frac{1}{2}0} &= H^S_{\frac{1}{2}0} - H^P_{\frac{1}{2}0},\\
H^S_{\frac{1}{2}0} &= G_S\frac{\sqrt{Q_+}}{m_b - m_c}[m_-f_1(q^2) + q^2f_3(q^2)],\\
H^P_{\frac{1}{2}0} &= G_S\frac{\sqrt{Q_-}}{m_b + m_c}[m_+g_1(q^2) - q^2g_3(q^2)].
\end{aligned} \tag{20}$$

For these amplitudes, the helicity flipped counterparts are $H^S_{-\lambda_2-\lambda_W} = H^S_{\lambda_2\lambda_W}$ and $H^P_{-\lambda_2-\lambda_W} = -H^P_{\lambda_2\lambda_W}$.

The form factors $f's$ and $g's$ can also be expressed in terms of the Isgur-Wise function $\zeta_1(w)$ as

$$\begin{aligned}
f_1(q^2) &= \zeta_1(w)\left[-\frac{1}{3} + m_+X_+\right],\\
f_2(q^2) &= \zeta_1(w)X_+,\\
f_3(q^2) &= \zeta_1(w)X_-,\\
g_1(q^2) &= \zeta_1(w)\left(-\frac{1}{3}\right),\\
g_2(q^2) &= 0,\\
g_3(q^2) &= 0.
\end{aligned} \tag{21}$$

Similarly, the helicity amplitudes in Eqs. (18) and (20) can be simplified in the following form:

$$\begin{aligned}
H^V_{\frac{1}{2}0} &= \zeta_1(w)G_V\frac{\sqrt{Q_-}}{\sqrt{q^2}}\left[m_+\left(-\frac{1}{3} + m_+X_+\right) - q^2X_+\right],\\
H^A_{\frac{1}{2}0} &= \zeta_1(w)G_A\frac{\sqrt{Q_+}}{\sqrt{q^2}}\left[-\frac{1}{3}m_-\right],\\
H^V_{\frac{1}{2}1} &= \zeta_1(w)G_V\sqrt{2Q_-}\left[\left(\frac{1}{3} - m_+X_+\right) + m_+X_+\right],\\
H^A_{\frac{1}{2}1} &= \zeta_1(w)G_A\sqrt{2Q_+}\left[\frac{1}{3}\right],\\
H^V_{\frac{1}{2}t} &= \zeta_1(w)G_V\frac{\sqrt{Q_+}}{\sqrt{q^2}}\left[m_-\left(-\frac{1}{3} + m_+X_+\right) + q^2X_-\right],\\
H^A_{\frac{1}{2}t} &= \zeta_1(w)G_A\frac{\sqrt{Q_-}}{\sqrt{q^2}}\left[-\frac{1}{3}m_+\right],\\
H^S_{\frac{1}{2}0} &= \zeta_1(w)G_S\frac{\sqrt{Q_+}}{m_b - m_c}\left[m_-\left(-\frac{1}{3} + m_+X_+\right) + q^2X_-\right],\\
H^P_{\frac{1}{2}0} &= \zeta_1(w)G_S\frac{\sqrt{Q_-}}{m_b + m_c}\left[-\frac{1}{3}m_+\right],
\end{aligned} \tag{23}$$

where $X_\pm = 2/[3(w+1)][m_\pm/m_{B_1}m_{B_2}]$.

B. Decay distribution and q^2 observables

To obtain the normalized differential decay rate, we perform the $\cos\theta$ integration in Eq. (9), i.e.,

$$\frac{d\Gamma}{dq^2} = \frac{8N}{3}\left(1 - \frac{m_l^2}{q^2}\right)^2\left[\mathcal{B}_1 + \frac{m_l^2}{2q^2}\mathcal{B}_2 + \frac{3}{2}\mathcal{B}_3 + \frac{3m_l}{\sqrt{q^2}}\mathcal{B}_4\right], \tag{24}$$

where

$$\begin{aligned}
\mathcal{B}_1 &= H^2_{\frac{1}{2}0} + H^2_{-\frac{1}{2}0} + H^2_{\frac{1}{2}1} + H^2_{-\frac{1}{2}-1},\\
\mathcal{B}_2 &= H^2_{\frac{1}{2}0} + H^2_{-\frac{1}{2}0} + H^2_{\frac{1}{2}1} + H^2_{-\frac{1}{2}-1} + 3\left(H^2_{\frac{1}{2}t} + H^2_{-\frac{1}{2}t}\right),\\
\mathcal{B}_3 &= \left(H^{SP}_{\frac{1}{2}0}\right)^2 + \left(H^{SP}_{-\frac{1}{2}0}\right)^2,\\
\mathcal{B}_4 &= H_{\frac{1}{2}t}H^{SP}_{\frac{1}{2}0} + H_{-\frac{1}{2}t}H^{SP}_{-\frac{1}{2}0}.
\end{aligned} \tag{25}$$

The SM equations can be obtained by setting $G_V = G_A = 1$ and $\tilde{G}_V = \tilde{G}_A = 0$.

The ratio of branching ratio is defined by considering the ratios of the differential decay rate with the heavier τ lepton in the final state to the differential decay rate with the corresponding lighter lepton in the final state as

$$R_{B_2} = \frac{\Gamma(B_1 \to B_2\tau\nu)}{\Gamma(B_1 \to B_2 l\nu)}, \tag{26}$$

where $B_{1(2)} = \Sigma_{b(c)}, \Omega_{b(c)}$ and $l = e$ or μ.

Similarly, we also define various q^2 dependent observables such as total differential decay rate $d\Gamma/dq^2(q^2)$, ratio of branching ratio $R_{B_2}(q^2)$, forward backward asymmetry $A^l_{FB}(q^2)$ obtained by integrating over linear $\cos\theta$ dependency of the distribution, and polarization fraction of the charged lepton $P^l(q^2)$ calculated by measuring the difference between the lepton helicity nonflip rate to the lepton helicity flip rate and convexity parameter $C^l_F(q^2)$ which is found by integrating over $\cos^2\theta$ dependency of the distribution for both of the decay modes as follows:

$$
\begin{aligned}
R_{B_2}(q^2) &= \frac{\Gamma(B_1 \to B_2 \tau \nu)}{\Gamma(B_1 \to B_2 l \nu)}, \\
A^l_{FB}(q^2) &= \frac{(\int_{-1}^{0} - \int_{0}^{1}) d\cos\theta \frac{d^2\Gamma}{dq^2 d\cos\theta}}{\frac{d\Gamma}{dq^2}}, \\
P^l(q^2) &= \frac{d\Gamma(+)/dq^2 - d\Gamma(-)/dq^2}{d\Gamma(+)/dq^2 + d\Gamma(-)/dq^2}, \\
C^l_F(q^2) &= \frac{1}{(d\Gamma/dq^2)} \frac{d^2}{d(\cos\theta)^2} \left[\frac{d^2\Gamma}{dq^2 d\cos\theta} \right],
\end{aligned} \tag{27}
$$

where $d\Gamma(+)/dq^2$ and $d\Gamma(-)/dq^2$ are the respective differential decay rates of positive and negative helicity of lepton. The average values of all the observables such as $\langle P^l \rangle$, $\langle A^l_{FB} \rangle$, $\langle C^l_F \rangle$, and $\langle R \rangle$ are obtained by integrating the numerator and denominator separately before taking the ratio.

III. RESULTS AND DISCUSSIONS

A. Input parameter

For our numerical computation of various observables we use the input parameters from Ref. [78] and, for definiteness, we report it in Table II. Masses of all the particles are in GeV units and Fermi coupling constant G_F is in GeV^{-2} unit. For the $\Sigma_b \to \Sigma_c$ and $\Omega_b \to \Omega_c$ transition form factors, we follow Ref. [56] and use the form factor inputs obtained in the framework of the relativistic quark model. In the heavy quark limit the invariant form factors are expressed in terms of the Isgur-Wise functions $\zeta_1(w)$ and $\zeta_2(w)$ obtained for the whole kinematic range using the $\Psi_{\Sigma_{(b,c)}}$ and $\Psi_{\Omega_{(b,c)}}$ baryon wave functions. The values of $\zeta_1(w)$ and $\zeta_2(w)$ in the whole kinematic range, pertinent for our analysis, were obtained from Ref. [79].

B. Standard model predictions

The SM predictions are reported for $\Sigma_b \to \Sigma_c l\nu$ and $\Omega_b \to \Omega_c l\nu$ decay modes undergoing $b \to c l\nu$ quark level transitions where l is either an electron or a tau lepton. In Table III, we display the average values of various observables such as the total decay rate Γ, longitudinal polarization of the charged lepton $\langle P^l \rangle$, forward-backward asymmetry $\langle A^l_{FB} \rangle$, and the convexity parameter $\langle C^l_F \rangle$ for both electron mode and tau mode respectively. We also report the ratio of branching ratios for these decay modes. The total decay rate for both the decay modes is observed to be larger for the lighter leptons (e or μ) as compared to the heavier τ lepton. The polarization fraction for the electron is

TABLE II. Theory input parameters [78].

Parameter	Value	Parameter	Value	Parameter	Value	Parameter	Value
m_{Σ_b}	5.8155	m_{Σ_c}	2.45375	$m_b(m_b)$	4.18	$m_c(m_b)$	0.91
m_{Ω_b}	6.0461	m_{Ω_c}	2.6952	G_F	1.1663787×10^{-5}	$\lvert V_{cb} \rvert$	0.041(11)
m_e	0.51099×10^{-3}	m_τ	1.77682				

TABLE III. The SM central values and the corresponding 1σ range for the total decay rate Γ, the ratio of branching ratio $\langle R \rangle$, the lepton polarization fraction $\langle P^l \rangle$, the forward-backward asymmetry $\langle A^l_{FB} \rangle$, and the convexity factor $\langle C^l_F \rangle$ for the e mode and the τ mode of $\Sigma_b \to \Sigma_c l\nu$ and $\Omega_b \to \Omega_c l\nu$ decays.

		$\Sigma_b \to \Sigma_c l\nu$		$\Omega_b \to \Omega_c l\nu$	
		e mode	τ mode	e mode	τ mode
$\Gamma \times 10^{10}$ s^{-1}	Central value	1.401	0.473	1.235	0.447
	1σ range (with 10% uncertainty in ζ_1)	[1.325, 1.474]	[0.447, 0.506]	[1.162, 1.284]	[0.422, 0.480]
	1σ range (with 20% uncertainty in ζ_1)	[1.259, 1.548]	[0.425, 0.538]	[1.113, 1.348]	[0.401, 0.514]
	1σ range (with 30% uncertainty in ζ_1)	[1.205, 1.631]	[0.406, 0.573]	[1.073, 1.422]	[0.382, 0.551]
$\langle P^l \rangle$	Central values	−1.000	0.131	−1.000	0.135
$\langle A^l_{FB} \rangle$	Central value	0.050	−0.253	0.050	−0.251
$\langle C^l_F \rangle$	Central value	−1.172	−0.200	−1.148	−0.196
$\langle R \rangle$	Central value	0.338		0.362	

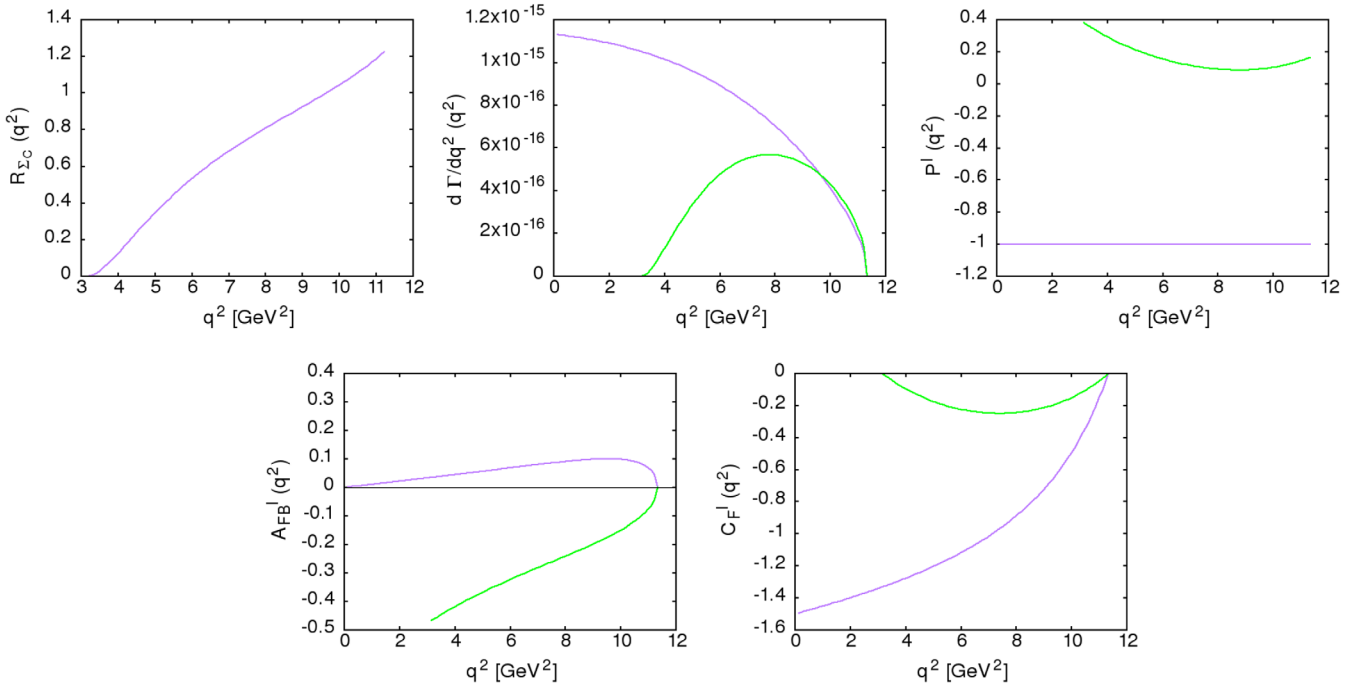

FIG. 3. Ratio of branching ratio $R_{\Sigma_c}(q^2)$, the total differential decay rate $d\Gamma/dq^2$, the lepton polarization fraction $P^l(q^2)$, the forward-backward asymmetry $A^l_{FB}(q^2)$, and the convexity parameter $C^l_F(q^2)$ for the $\Sigma_b \to \Sigma_c l\nu$ decays in the SM. The purple color represents the e mode and the green color represents the τ mode.

-1.00. The τ polarization fraction is 0.131 for $\Sigma_b \to \Sigma_c$ and 0.135 for $\Omega_b \to \Omega_c$ decay modes. The forward-backward asymmetry for electron mode and tau mode are almost similar for both the decay modes. The convexity parameter C^l_F for the τ mode is larger than the e mode. The ratio of branching ratio for $\Omega_b \to \Omega_c l\nu$ is slightly larger than the $\Sigma_b \to \Sigma_c l\nu$ decay mode.

We also determine the size of uncertainties in each observable that are coming from various input parameters. The uncertainties for the theoretical predictions can come from the nonperturbative hadronic form factors and not very well-know Cabibbo–Kobayashi–Maskawa (CKM) matrix element $|V_{cb}|$. Here, we consider the 10% uncertainty in $\zeta_1(w)$ and the $|V_{cb}|$ uncertainty as mentioned in Table II. In order to measure the size of uncertainty, we perform a random scan over the input parameters within 1σ. Although, the assumption of 10% uncertainty in the form factor inputs is conservative, if one assumes it to be even larger than 10% i.e., 20% or 30%, it is not going to affect the results severely. We see that, except for Γ, the form factor uncertainty exactly cancels in all the other observables. In Table III, we report the uncertainty range for Γ with 10%, 20%, and 30% uncertainty in the form factors. We see that there is no uncertainty in $\langle P^l \rangle$, $\langle A^l_{FB} \rangle$, $\langle C^l_F \rangle$, and $\langle R \rangle$.

The behavior of each observable as a function of q^2 for $\Sigma_b \to \Sigma_c l\nu$ and $\Omega_b \to \Omega_c l\nu$ decays are reported in Figs. 3 and 4. We compare each observable for both electron and tau lepton final states. Purple represents the electron mode and green represents the tau mode. The q^2 dependence of all of the observables are distinct for both e and τ modes. The $R_{\Sigma_c}(q^2)$ show an almost positive slope over the entire q^2 range. The total differential decay rate for electron is maximum at minimum q^2 and minimum at maximum q^2 whereas, the total differential decay rate for tau is maximum at around $q^2 = 8$ GeV^2 and approaches zero at minimum and maximum q^2. The $P^e(q^2)$ is -1 over the entire q^2 range and the $P^\tau(q^2)$ take only positive values for all q^2 values. The $A^l_{FB}(q^2)$ is positive in e mode while it is negative in τ mode in the whole q^2 range. At $q^2 = q^2_{\rm max}$, both $A^e_{FB}(q^2)$ and $A^\tau_{FB}(q^2)$ approach to zero. The $C^e_F(q^2)$ is around -1.5 at $q^2 = m^2_l$ and zero at maximum q^2. On the other hand $C^\tau_F(q^2)$ approaches zero at both minimum and maximum q^2. Similar conclusions can be made for the $\Omega_b \to \Omega_c l\nu$ decay mode as well.

C. New physics analysis

We analyze the NP effects in a model independent way. The new physics effects are investigated in four different scenarios by considering each new vector and scalar type NP couplings associated with the left-handed neutrinos one at a time. The effects of V_L, V_R, S_L, and S_R NP couplings are studied for both $\Sigma_b \to \Sigma_c \tau\nu$ and $\Omega_b \to \Omega_c \tau\nu$ decay modes. We first perform a naive χ^2 test to find the best fit values of each observable by defining

$$[\chi^2]_{\rm Total} = \frac{[R^{\rm expt}_D - R^{\rm th}_D]^2}{[\Delta R^{\rm expt}_D]^2} + \frac{[R^{\rm expt}_{D^*} - R^{\rm th}_{D^*}]^2}{[\Delta R^{\rm expt}_{D^*}]^2} \qquad (28)$$

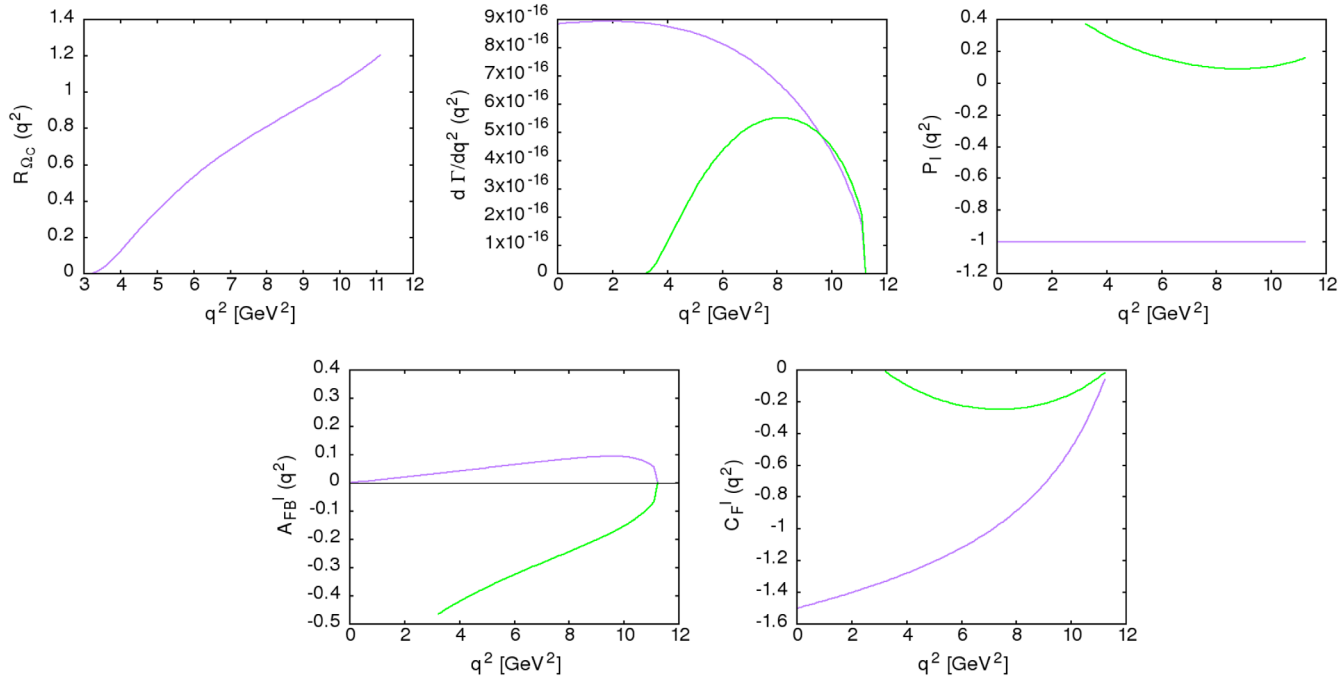

FIG. 4. Ratio of branching ratio $R_{\Omega_c}(q^2)$, the total differential decay rate $d\Gamma/dq^2$, the lepton polarization fraction $P^l(q^2)$, the forward-backward asymmetry $A^l_{FB}(q^2)$, and the convexity parameter $C^l_F(q^2)$ as a function of q^2 for the $\Omega_b \to \Omega_c l\nu$ decays in the SM. Purple represents the e mode and green represents the τ mode.

where, $R_D^{\rm expt}$ and $R_{D^*}^{\rm expt}$ refer to the experimental values of R_D and R_{D^*} and $\Delta R_D^{\rm expt}$, $\Delta R_{D^*}^{\rm expt}$ refer to the experimental uncertainties associated with R_D and R_{D^*} and similarly $R_D^{\rm th}$, $R_{D^*}^{\rm th}$ refer to the theoretical values corresponding to various NP couplings. For the uncertainties in R_D and R_{D^*}, we added the systematic and statistical uncertainties in quadrature. To calculate the best fit values, we evaluate the minimum χ^2 and find the respective best fit values for each V_L, V_R, S_L, and S_R NP couplings. In Table IV, we display the corresponding best fit average values of each observable associated with V_L, V_R, S_L, and S_R NP couplings for the $\Sigma_b \to \Sigma_c\tau\nu$ and $\Omega_b \to \Omega_c\tau\nu$ decay modes. Although there are deviations of each observable in each NP scenarios, the forward-backward asymmetry $\langle A^\tau_{FB}\rangle$ corresponding to S_L shows a completely different pattern for both $\Sigma_b \to \Sigma_c\tau\nu$ and $\Omega_b \to \Omega_c\tau\nu$ decay modes. It assumes positive values for S_L and negative for the rest of the NP couplings. Measurement of $\langle A^\tau_{FB}\rangle$ for these decay modes in the future will be crucial in distinguishing various NP Lorentz structures. We also compare in Figs. 5 and 6 various q^2 dependent observables obtained using the best fit values of each NP couplings with the SM central value. It is evident that the deviation observed with the S_L NP coupling is quite different from all the other NP couplings in both the decay modes.

To get the allowed NP parameter space in each scenario, we impose the 3σ constraint coming from the measured values of the ratio of branching ratios R_D and R_{D^*}. We have shown in Fig. 7 the allowed ranges of V_L, V_R, S_L, and S_R NP couplings that are compatible with the 3σ constraints coming from the measured values of R_D and R_{D^*}. The allowed ranges of V_L, V_R, S_L, and S_R NP couplings are as follows:

TABLE IV. Ratio of branching ratio $\langle R\rangle$, the total decay rate Γ, the tau polarization fraction $\langle P^\tau\rangle$, the forward-backward asymmetry $\langle A^\tau_{FB}\rangle$, and the convexity parameter $\langle C^\tau_F\rangle$ for $\Sigma_b \to \Sigma_c\tau\nu$ and $\Omega_b \to \Omega_c\tau\nu$ decay modes with the best fit value of each NP coupling.

	$\Sigma_b \to \Sigma_c\tau\nu$				$\Omega_b \to \Omega_c\tau\nu$			
	V_L	V_R	S_L	S_R	V_L	V_R	S_L	S_R
$\Gamma \times 10^{10}$ s^{-1}	0.548	0.450	0.489	0.538	0.518	0.426	0.466	0.509
$\langle P^\tau\rangle$	0.131	0.092	0.159	0.236	0.135	0.095	0.170	0.241
$\langle A^\tau_{FB}\rangle$	−0.253	−0.241	0.242	−0.250	−0.251	−0.239	0.240	−0.248
$\langle C^\tau_F\rangle$	−0.200	−0.192	−0.193	−0.176	−0.196	−0.189	−0.188	−0.172
$\langle R\rangle$	0.391	0.321	0.349	0.384	0.419	0.345	0.377	0.421

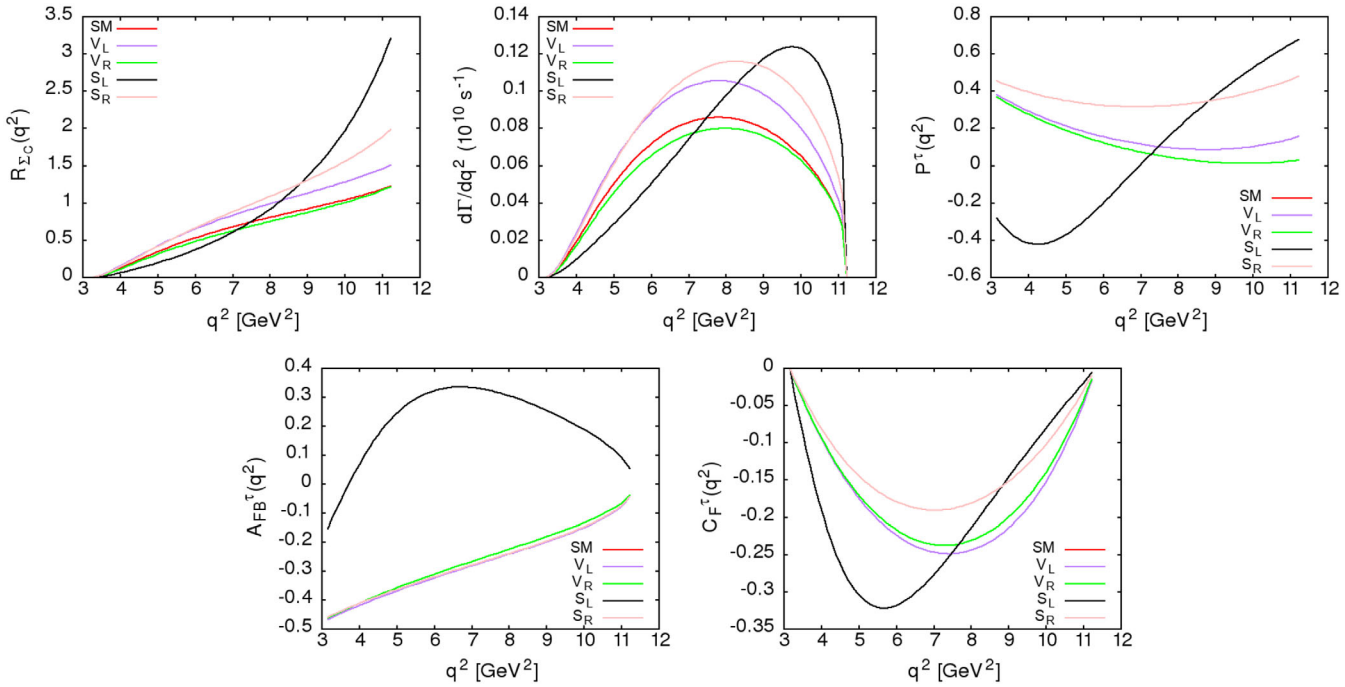

FIG. 5. The q^2 dependency of the ratio of branching ratio $R_{\Sigma_c}(q^2)$, the total differential decay rate $d\Gamma/dq^2$, the lepton polarization fraction $P^\tau(q^2)$, the forward-backward asymmetry $A^\tau_{FB}(q^2)$, and the convexity factor $C^\tau_F(q^2)$ in SM (red) and in the presence of V_L (purple), V_R (green), S_L (black), and S_R (pink) NP couplings for the $\Sigma_b \to \Sigma_c \tau\nu$ decay mode.

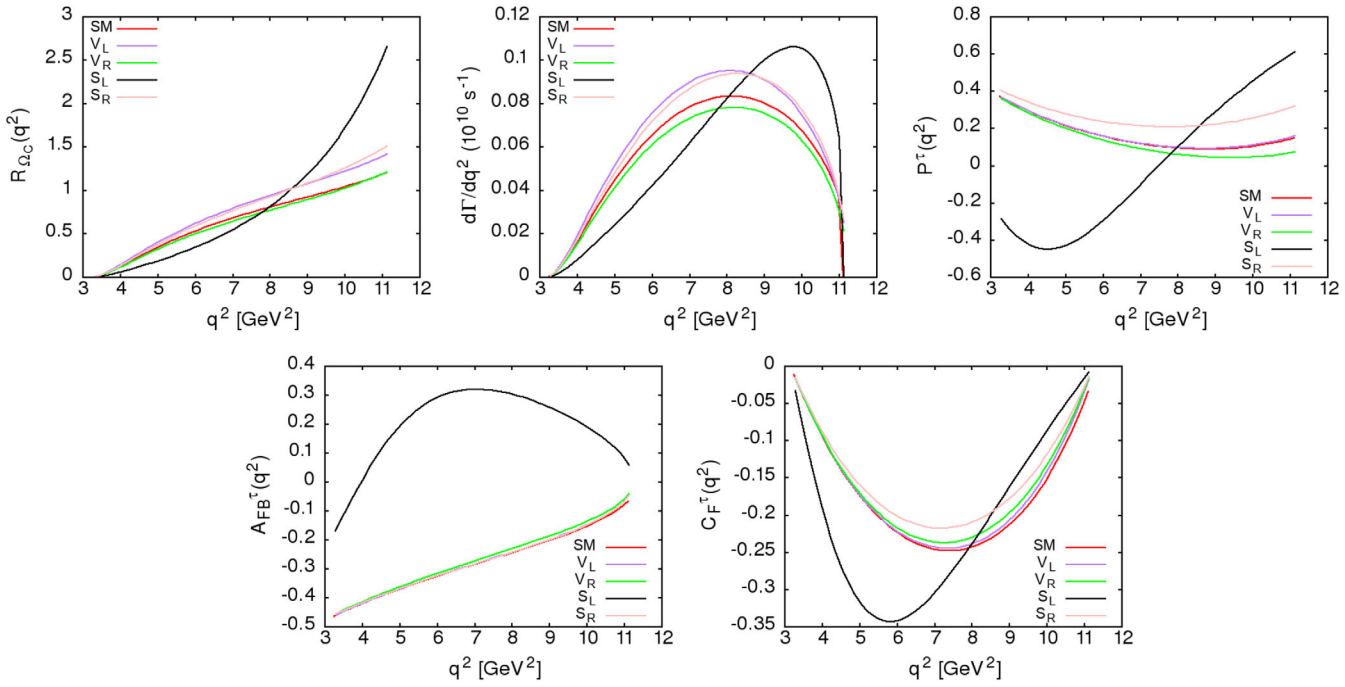

FIG. 6. The q^2 dependency of the ratio of branching ratio $R_{\Omega_c}(q^2)$, the total differential decay rate $d\Gamma/dq^2$, the lepton polarization fraction $P^\tau(q^2)$, the forward-backward asymmetry $A^\tau_{FB}(q^2)$, and the convexity factor $C^\tau_F(q^2)$ in SM (red) and in the presence of V_L (purple), V_R (green), S_L (black), and S_R (pink) NP couplings for the $\Omega_b \to \Omega_c \tau\nu$ decay mode.

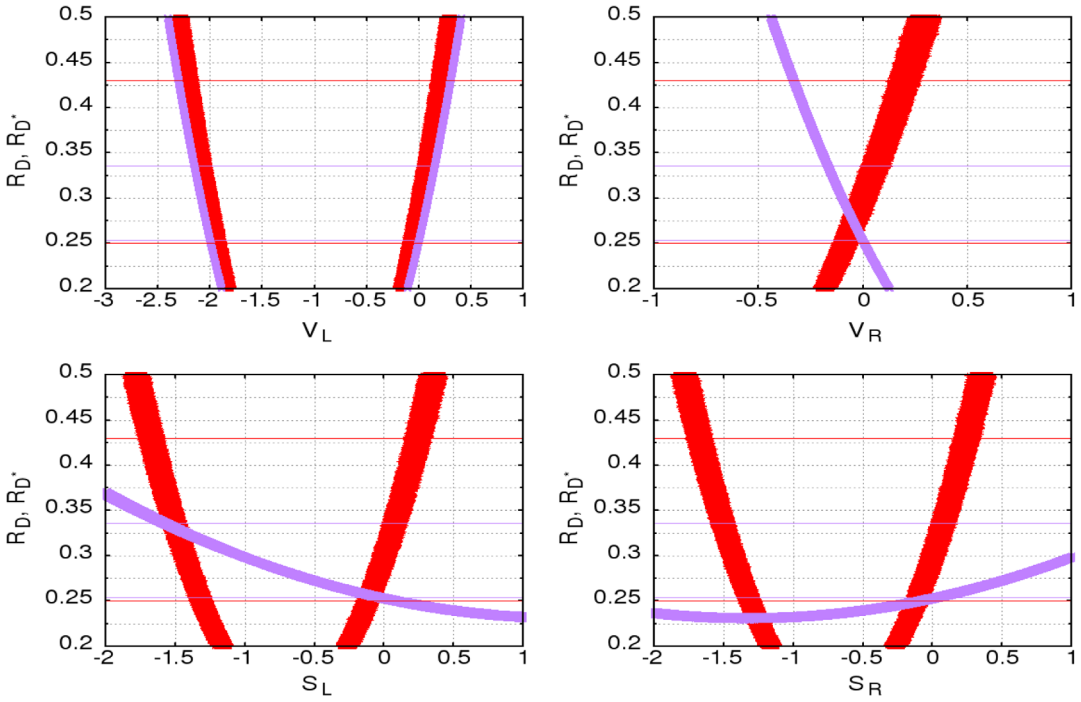

FIG. 7. The allowed regions of V_L, V_R, S_L, and S_R NP couplings once the 3σ constraint coming from the measured values of the ratio of branching ratios R_D and R_{D^*} are applied. Red represents R_D and purple represents R_{D^*}. The 3σ range for R_D is [0.2503, 0.4297] and R_{D^*} is [0.2542, 0.3358].

$$V_L \in [-0.2, 0.2], \qquad V_R \in [-0.1, 0.02],$$
$$S_L \in [-0.2, 0.1] \quad \text{and} \quad [-1.6, -1.4],$$
$$S_R \in [-0.2, 0.33]. \tag{29}$$

We also report the q^2 dependency of each observable such as the ratio of branching ratio $R_{\Sigma_c}(q^2)$ and $R_{\Omega_c}(q^2)$, the total differential decay rate $d\Gamma/dq^2$, the tau polarization fraction $P^\tau(q^2)$, the forward-backward asymmetry $A^\tau_{FB}(q^2)$, and the convexity factor $C^\tau_F(q^2)$ for both the decay modes in Figs. 8 and 9. In each figure we incorporate both SM and NP behavior. The SM and NP are distinguished by red and purple colors respectively. We represent the SM central curve and the corresponding 1σ band which we obtain by varying the input parameters (form factors and V_{cb}) within 1σ with red. On the other hand, the best fit curve and the band for each NP coupling obtained by imposing the 3σ constraint coming from the measured values of R_D and R_{D^*} are represented with purple. Our main observations are as follows:

(i) The effect of the V_L NP coupling is encoded in the vector and axial vector helicity amplitudes only. In case of $\Sigma_b \to \Sigma_c \tau\nu$ decays, the deviation from the SM prediction due to the V_L NP coupling is observed only in the ratio of branching ratio $R(q^2)$ and the total differential decay rate $d\Gamma/dq^2$. With V_L NP coupling the differential decay width $d\Gamma/dq^2$ is proportional to $(1+V_L)^2$. Hence, the NP dependency cancels in the ratios and we do not see any deviation from the Standard Model prediction for the observables such as $P^\tau(q^2)$, $A^\tau_{FB}(q^2)$, and $C^\tau_F(q^2)$. Similar conclusions can be made for the $\Omega_b \to \Omega_c \tau\nu$ decay mode as well.

(ii) Similar to V_L, the V_R NP effects are encoded in the vector and the axial vector helicity amplitudes alone. Deviation in each observable from the SM prediction is observed in this scenario. There is no cancellation of NP effects in $P^\tau(q^2)$, $A^\tau_{FB}(q^2)$, and $C^\tau_F(q^2)$ since, in the presence of the V_R NP coupling, $d\Gamma/dq^2$ depends on both $(1+V_R)^2$ and $(1-V_R)^2$. So there is no cancellation of NP effects in the ratios. As a result, we see deviation from the SM prediction in each observable. The deviation observed in $d\Gamma/dq^2$, $R(q^2)$, $A^\tau_{FB}(q^2)$, and $C^\tau_F(q^2)$ are less in comparison to the deviation observed in the tau polarization fraction $P^\tau(q^2)$. Similar conclusions can be made for the $\Omega_b \to \Omega_c \tau\nu$ decay mode as well.

(iii) The scalar NP coupling S_L comes into the decay amplitude through the scalar and pseudoscalar helicity amplitudes. In this scenario, the differential decay width $d\Gamma/dq^2$ depends on S_L linearly as well as quadratically, i.e., $d\Gamma/dq^2 \propto (S_L, S_L^2)$. Hence the NP dependency does not cancel in the ratios and we observe deviation of all the observables from the SM prediction. We even observe that the deviation from the SM prediction is more pronounced than that with V_L, V_R, and S_R NP couplings. This can be

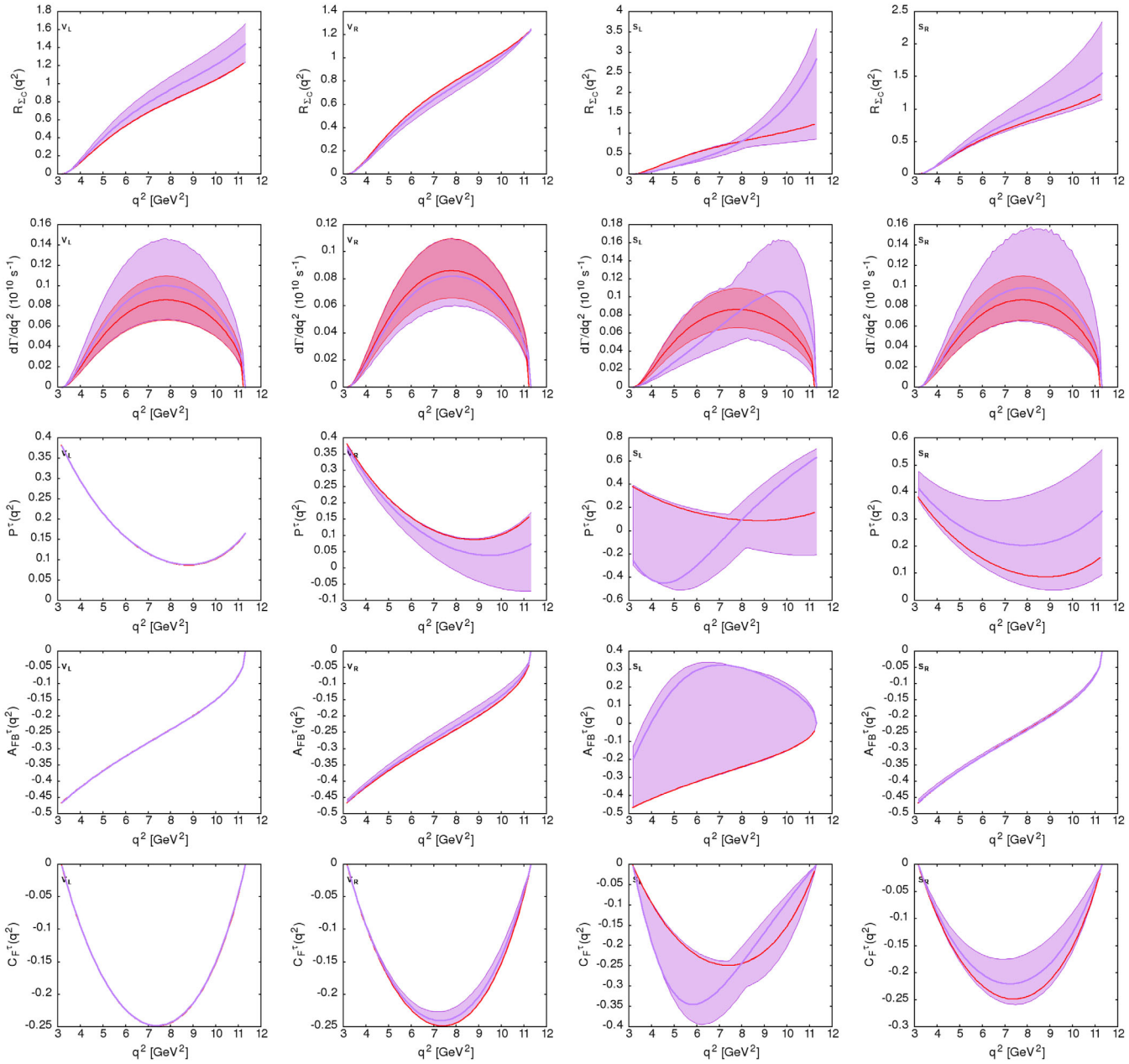

FIG. 8. The q^2 dependency of various observables such as the ratio of branching ratio $R_{\Sigma_c}(q^2)$, the total differential decay rate $d\Gamma/dq^2$, the tau polarization fraction $P^\tau(q^2)$, the forward-backward asymmetry $A_{FB}^\tau(q^2)$, and the convexity parameter $C_F^\tau(q^2)$ for the $\Sigma_b \to \Sigma_c \tau\nu$ decay mode in the presence of V_L (first column), V_R (second column), S_L (third column), and S_R (fourth column). NP couplings are shown with the purple band, whereas the SM prediction is shown with the red band. The red solid line represents the SM prediction with the central values of each input parameter and the purple solid line represents the prediction once the best fit values of the NP couplings are used.

easily understood from the allowed ranges of V_L, V_R, S_L, and S_R NP couplings. The strength of the S_L NP coupling is more than all the other NP couplings and accordingly, we see significantly wider bands than the SM plots in the scenario with the S_L NP coupling. More interestingly, the SM central curve and the best fit curve due to the S_L NP coupling show completely different behavior for all the observables. Moreover, there is even a zero crossing in the best fit curve of the tau polarization fraction $P^\tau(q^2)$ at $q^2 \approx 7.5\ \text{GeV}^2$ below which $P^\tau(q^2)$ takes negative values. Similarly, the best fit curve of forward-backward asymmetry $A_{FB}^\tau(q^2)$ has a zero crossing around $q^2 \approx 3.5\ \text{GeV}^2$. However, depending on the value of the S_L NP coupling, there may or may not be any zero crossing in $P^\tau(q^2)$ and $A_{FB}^\tau(q^2)$.

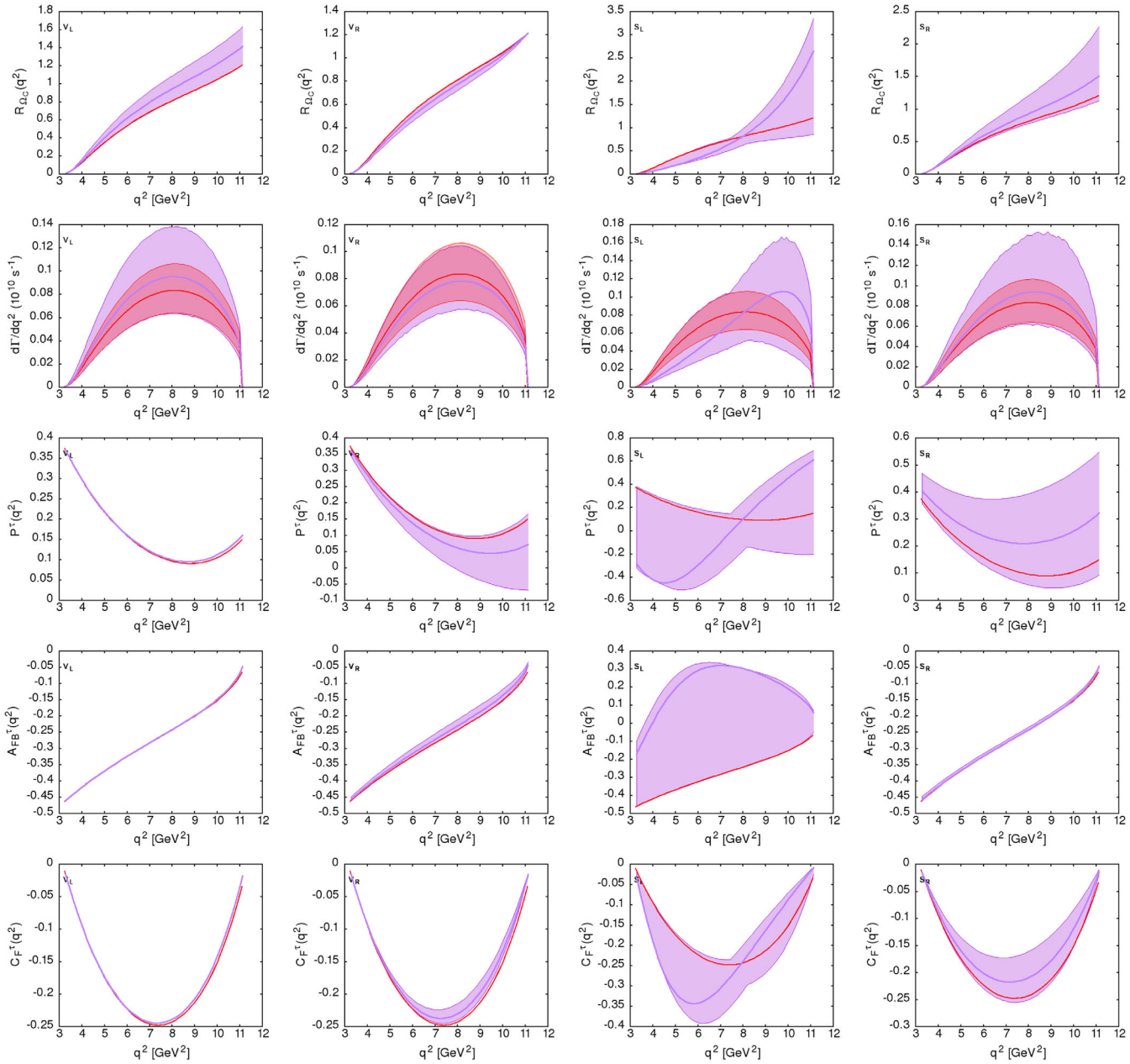

FIG. 9. The q^2 dependency of various observables such as the ratio of branching ratio $R_{\Sigma_c}(q^2)$, the total differential decay rate $d\Gamma/dq^2$, the tau polarization fraction $P^\tau(q^2)$, the forward-backward asymmetry $A_{FB}^\tau(q^2)$, and the convexity parameter $C_F^\tau(q^2)$ for the $\Omega_b \to \Omega_c \tau\nu$ decay mode in the presence of V_L (first column), V_R (second column), S_L (third column), and S_R (fourth column). NP couplings are shown with the purple band, whereas the SM prediction is shown with the red band. The red solid line represents the SM prediction with the central values of each input parameter and the purple solid line represents the prediction once the best fit values of the NP couplings are used.

(iv) Similar to S_L, NP effects coming from the S_R NP coupling are encoded in the scalar and pseudoscalar helicity amplitudes only. Again a significant deviation from the SM prediction is observed, in particular, for $R(q^2)$, $d\Gamma/dq^2$, $P^\tau(q^2)$, and $C_F^\tau(q^2)$ as the differential decay width $d\Gamma/dq^2$ depends on S_R linearly as well as quadratically, i.e., $d\Gamma/dq^2 \propto (S_R, S_R^2)$. Hence, the NP dependency does not cancel in the ratios. It is, however, worth mentioning that the NP effect in $A_{FB}(q^2)$ is quite negligible in this scenario.

IV. SUMMARY AND CONCLUSION

The main objective of this work is to determine the size of the lepton flavor universality violation in the semileptonic decays of Σ_b and Ω_b heavy baryons. Motivated by

the long-standing flavor anomalies in $B \to D^{(*)} l\nu$ decay modes, we follow a model independent effective field theory approach and study the various physical observables within the SM and in the presence of new vector and scalar type NP couplings. We have used the helicity formalism to construct the angular decay distribution for the $b \to c l\nu$ transitions. We define several observables such as the lepton polarization, lepton side forward-backward asymmetry, and convexity parameter for the $\Sigma_b \to \Sigma_c l\nu$ and $\Omega_b \to \Omega_c l\nu$ decays. The numerical results have been presented for both electron mode and tau mode within the SM. We also display the q^2 dependant plots within the SM and within various NP scenarios. To find the allowed parameter space, we impose a 3σ constraint coming from the measured ratio of branching ratios R_D and R_{D^*}. We perform our analysis by considering each NP parameter one at time. We also perform a naive χ^2 analysis to determine the best fit values of each NP coupling. The corresponding best fit values of each observable are also reported. The deviation observed with scalar NP couplings is more pronounced than that with the vector NP couplings. The deviation observed in the case of the S_L NP coupling is quite distinct from all other NP couplings. In the future, this may help to identify the exact nature of NP.

Unlike B meson decays which have been rigorously studied both theoretically and experimentally over the last decade, the baryonic decay modes which undergo similar quark level transitions are less explored. Study of these decay modes are useful for two reasons. First, it can provide us complementary information regarding NP in various B meson decays and also can be useful in determining the value of the CKM matrix element $|V_{cb}|$. Second, study of these decay modes both theoretically and experimentally can act as a useful ingredient in maximizing future sensitivity to NP.

ACKNOWLEDGMENTS

We are grateful to D. Ebert, R. N. Faustov, and V. O. Galkin for providing us the Isgur-Wise functions $\zeta_1(w)$ and $\zeta_2(w)$ in the whole kinematic range used for computing $\Sigma_b \to \Sigma_c$ and $\Omega_b \to \Omega_c$ transition form factors.

[1] M. Ida and R. Kobayashi, Baryon resonances in a quark model, Prog. Theor. Phys. **36**, 846 (1966).
[2] D. B. Lichtenberg and L. J. Tassie, Baryon mass splitting in a Boson-Fermion model, Phys. Rev. **155**, 1601 (1967).
[3] M. Anselmino, E. Predazzi, S. Ekelin, S. Fredriksson, and D. B. Lichtenberg, Diquarks, Rev. Mod. Phys. **65**, 1199 (1993).
[4] J. A. Bailey *et al.* (MILC Collaboration), BD form factors at nonzero recoil and $|V_{cb}|$ from $2+1$-flavor lattice QCD, Phys. Rev. D **92**, 034506 (2015).
[5] H. Na, C. M. Bouchard, G. P. Lepage, C. Monahan, and J. Shigemitsu (HPQCD Collaboration), $B \to Dl\nu$ form factors at nonzero recoil and extraction of $|V_{cb}|$, Phys. Rev. D **92**, 054510 (2015); Erratum, Phys. Rev. D **93**, 119906(E) (2016).
[6] S. Aoki *et al.*, Review of lattice results concerning low-energy particle physics, Eur. Phys. J. C **77**, 112 (2017).
[7] D. Bigi and P. Gambino, Revisiting $B \to D\ell\nu$, Phys. Rev. D **94**, 094008 (2016).
[8] F. U. Bernlochner, Z. Ligeti, M. Papucci, and D. J. Robinson, Combined analysis of semileptonic B decays to D and D^*: $R(D^{(*)})$, $|V_{cb}|$, and new physics, Phys. Rev. D **95**, 115008 (2017); Erratum, Phys. Rev. D **97**, 059902(E) (2018).
[9] S. Jaiswal, S. Nandi, and S. K. Patra, Extraction of $|V_{cb}|$ from $B \to D^{(*)}\ell\nu_\ell$ and the standard model predictions of $R(D^{(*)})$, J. High Energy Phys. 12 (2017) 060.
[10] S. Fajfer, J. F. Kamenik, and I. Nisandzic, On the $B \to D^*\tau\bar{\nu}_\tau$ sensitivity to new physics, Phys. Rev. D **85**, 094025 (2012).
[11] D. Bigi, P. Gambino, and S. Schacht, $R(D^*)$, $|V_{cb}|$, and the heavy quark symmetry relations between form factors, J. High Energy Phys. 11 (**2017**) 061.
[12] A. Abdesselam *et al.* (Belle Collaboration), Precise determination of the CKM matrix element $|V_{cb}|$ with $\bar{B}^0 \to D^{*+}\ell^-\bar{\nu}_\ell$ decays with hadronic tagging at Belle, arXiv:1702.01521.
[13] J. P. Lees *et al.* (*BABAR* Collaboration), Measurement of an excess of $\bar{B} \to D^{(*)}\tau^-\bar{\nu}_\tau$ decays and implications for charged Higgs bosons, Phys. Rev. D **88**, 072012 (2013).
[14] J. P. Lees *et al.* (*BABAR* Collaboration), Evidence for an Excess of $\bar{B} \to D^{(*)}\tau^-\bar{\nu}_\tau$ Decays, Phys. Rev. Lett. **109**, 101802 (2012).
[15] M. Huschle *et al.* (Belle Collaboration), Measurement of the branching ratio of $\bar{B} \to D^{(*)}\tau^-\bar{\nu}_\tau$ relative to $\bar{B} \to D^{(*)}\ell^-\bar{\nu}_\ell$ decays with hadronic tagging at Belle, Phys. Rev. D **92**, 072014 (2015).
[16] A. Abdesselam *et al.* (Belle Collaboration), Measurement of $\mathcal{R}(D)$ and $\mathcal{R}(D^*)$ with a semileptonic tagging method, arXiv:1904.08794.
[17] Y. Sato *et al.* (Belle Collaboration), Measurement of the branching ratio of $\bar{B}^0 \to D^{*+}\tau^-\bar{\nu}_\tau$ relative to $\bar{B}^0 \to D^{*+}\ell^-\bar{\nu}_\ell$ decays with a semileptonic tagging method, Phys. Rev. D **94**, 072007 (2016).
[18] S. Hirose *et al.* (Belle Collaboration), Measurement of the τ Lepton Polarization and $R(D^*)$ in the Decay $\bar{B} \to D^*\tau^-\bar{\nu}_\tau$, Phys. Rev. Lett. **118**, 211801 (2017).
[19] S. Hirose *et al.* (Belle Collaboration), Measurement of the τ lepton polarization and $R(D^*)$ in the decay $\bar{B} \to D^*\tau^-\bar{\nu}_\tau$

with one-prong hadronic τ decays at Belle, Phys. Rev. D **97**, 012004 (2018).
[20] R. Aaij *et al.* (LHCb Collaboration), Measurement of the Ratio of Branching Fractions $\mathcal{B}(\bar{B}^0 \to D^{*+}\tau^-\bar{\nu}_\tau)/\mathcal{B}(\bar{B}^0 \to D^{*+}\mu^-\bar{\nu}_\mu)$, Phys. Rev. Lett. **115**, 111803 (2015); Erratum, Phys. Rev. Lett. **115**, 159901(E) (2015).
[21] R. Aaij *et al.* (LHCb Collaboration), Measurement of the Ratio of the $B^0 \to D^{*-}\tau^+\nu_\tau$ and $B^0 \to D^{*-}\mu^+\nu_\mu$ Branching Fractions Using Three-Prong τ-Lepton Decays, Phys. Rev. Lett. **120**, 171802 (2018).
[22] R. Aaij *et al.* (LHCb Collaboration), Test of lepton flavor universality by the measurement of the $B^0 \to D^{*-}\tau^+\nu_\tau$ branching fraction using three-prong τ decays, Phys. Rev. D **97**, 072013 (2018).
[23] Y. Sakaki, M. Tanaka, A. Tayduganov, and R. Watanabe, Probing new physics with q^2 distributions in $\bar{B} \to D^{(*)}\tau\bar{\nu}$, Phys. Rev. D **91**, 114028 (2015).
[24] M. Freytsis, Z. Ligeti, and J. T. Ruderman, Flavor models for $\bar{B} \to D^{(*)}\tau\bar{\nu}$, Phys. Rev. D **92**, 054018 (2015).
[25] S. Bhattacharya, S. Nandi, and S. K. Patra, Looking for possible new physics in $B \to D^{(*)}\tau\nu_\tau$ in light of recent data, Phys. Rev. D **95**, 075012 (2017).
[26] A. K. Alok, D. Kumar, J. Kumar, S. Kumbhakar, and S. U. Sankar, New physics solutions for R_D and R_{D^*}, J. High Energy Phys. 09 (2018) 152.
[27] A. Azatov, D. Bardhan, D. Ghosh, F. Sgarlata, and E. Venturini, Anatomy of $b \to c\tau\nu$ anomalies, J. High Energy Phys. 11 (2018) 187.
[28] S. Bifani, S. Descotes-Genon, A. R. Vidal, and M. H. Schune, Review of lepton universality tests in B decays, J. Phys. G **46**, 023001 (2019).
[29] Z. R. Huang, Y. Li, C. D. Lu, M. A. Paracha, and C. Wang, Footprints of new physics in $b \to c\tau\nu$ transitions, Phys. Rev. D **98**, 095018 (2018).
[30] Q. Y. Hu, X. Q. Li, and Y. D. Yang, $b \to c\tau\nu$ transitions in the standard model effective field theory, Eur. Phys. J. C **79**, 264 (2019).
[31] F. Feruglio, P. Paradisi, and O. Sumensari, Implications of scalar and tensor explanations of $R_{D^{(*)}}$, J. High Energy Phys. 11 (2018) 191.
[32] S. Iguro, Y. Omura, and M. Takeuchi, Test of the $R(D^{(*)})$ anomaly at the LHC, Phys. Rev. D **99**, 075013 (2019).
[33] M. Jung and D. M. Straub, Constraining new physics in $b \to c\ell\nu$ transitions, J. High Energy Phys. 01 (2019) 009.
[34] A. Datta, S. Kamali, S. Meinel, and A. Rashed, Phenomenology of $\Lambda_b \to \Lambda_c\tau\bar{\nu}_\tau$ using lattice QCD calculations, J. High Energy Phys. 08 (**2017**) 131.
[35] R. Dutta and N. Rajeev, Signature of lepton flavor universality violation in $B_s \to D_s\tau\nu$ semileptonic decays, Phys. Rev. D **97**, 095045 (2018).
[36] F. U. Bernlochner, Z. Ligeti, D. J. Robinson, and W. L. Sutcliffe, New Predictions for $\Lambda_b \to \Lambda_c$ Semileptonic Decays and Tests of Heavy Quark Symmetry, Phys. Rev. Lett. **121**, 202001 (2018).
[37] R. Dutta and A. Bhol, $B_c \to (J/\psi, \eta_c)\tau\nu$ semileptonic decays within the standard model and beyond, Phys. Rev. D **96**, 076001 (2017).
[38] A. K. Alok, D. Kumar, S. Kumbhakar, and S. U. Sankar, Resolution of R_D/R_{D^*} puzzle, Phys. Lett. B **784**, 16 (2018).
[39] R. Dutta, Predictions of $B_c \to (D, D^*)\tau\nu$ decay observables in the standard model, J. Phys. G **46**, 035008 (2019).
[40] W. Altmannshofer, P. S. B. Dev, and A. Soni, $R_{D^{(*)}}$ anomaly: A possible hint for natural supersymmetry with R-parity violation, Phys. Rev. D **96**, 095010 (2017).
[41] M. Blanke, A. Crivellin, S. de Boer, T. Kitahara, M. Moscati, U. Nierste, and I. Niandi, Impact of polarization observables and $B_c \to \tau\nu$ on new physics explanations of the $b \to c\tau\nu$ anomaly, Phys. Rev. D **99**, 075006 (2019).
[42] M. Blanke, A. Crivellin, T. Kitahara, M. Moscati, U. Nierste, and I. Niandi, Addendum: Impact of polarization observables and $B_c \to \tau\nu$ on new physics explanations of the $b \to c\tau\nu$ anomaly, arXiv:1905.08253.
[43] S. Fajfer, J. F. Kamenik, I. Nisandzic, and J. Zupan, Implications of Lepton Flavor Universality Violations in B Decays, Phys. Rev. Lett. **109**, 161801 (2012).
[44] A. Crivellin, C. Greub, and A. Kokulu, Explaining $B \to D\tau\nu$, $B \to D^*\tau\nu$ and $B \to \tau\nu$ in a 2HDM of type III, Phys. Rev. D **86**, 054014 (2012).
[45] X. Q. Li, Y. D. Yang, and X. Zhang, Revisiting the one leptoquark solution to the $R(\mathrm{D}^{(})$ anomalies and its phenomenological implications, J. High Energy Phys. 08 (2016) 054.
[46] D. Bardhan, P. Byakti, and D. Ghosh, A closer look at the R_D and R_{D^*} anomalies, J. High Energy Phys. 01 (2017) 125.
[47] A. K. Alok, D. Kumar, S. Kumbhakar, and S. U. Sankar, D^* polarization as a probe to discriminate new physics in $\bar{B} \to D^*\tau\bar{\nu}$, Phys. Rev. D **95**, 115038 (2017).
[48] R. Dutta and A. Bhol, $b \to (c, u), \tau\nu$ leptonic and semileptonic decays within an effective field theory approach, Phys. Rev. D **96**, 036012 (2017).
[49] R. Dutta, Exploring R_D, R_{D^*} and $R_{J/\Psi}$ anomalies, arXiv:1710.00351.
[50] B. Bhattacharya, A. Datta, J. P. Guvin, D. London, and R. Watanabe, Simultaneous explanation of the R_K and $R_{D^{(*)}}$ puzzles: A model analysis, J. High Energy Phys. 01 (2017) 015.
[51] R. Dutta, $\Lambda_b \to (\Lambda_c, p)\tau\nu$ decays within standard model and beyond, Phys. Rev. D **93**, 054003 (2016).
[52] N. Rajeev and R. Dutta, Impact of vector new physics couplings on $B_s \to (K, K^*)\tau\nu$ and $B \to \pi\tau\nu$ decays, Phys. Rev. D **98**, 055024 (2018).
[53] A. K. Alok, D. Kumar, S. Kumbhakar, and S. U. Sankar, Impact of D^* polarization measurement on solutions to $R_D - R_{D^*}$ anomalies, arXiv:1903.10486.
[54] R. Aaij *et al.* (LHCb Collaboration), Measurement of the Ratio of Branching Fractions $\mathcal{B}(B_c^+ \to J/\psi\tau^+\nu_\tau)/\mathcal{B}(B_c^+ \to J/\psi\mu^+\nu_\mu)$, Phys. Rev. Lett. **120**, 121801 (2018).
[55] T. D. Cohen, H. Lamm, and R. F. Lebed, Model-independent bounds on $R(J/\psi)$, J. High Energy Phys. 09 (2018) 168.
[56] D. Ebert, R. N. Faustov, and V. O. Galkin, Semileptonic decays of heavy baryons in the relativistic quark model, Phys. Rev. D **73**, 094002 (2006).
[57] R. L. Singleton, Semileptonic baryon decays with a heavy quark, Phys. Rev. D **43**, 2939 (1991).
[58] M. A. Ivanov, V. E. Lyubovitskij, J. G. Korner, and P. Kroll, Heavy baryon transitions in a relativistic three quark model, Phys. Rev. D **56**, 348 (1997).

[59] M. A. Ivanov, J. G. Korner, V. E. Lyubovitskij, and A. G. Rusetsky, Charm and bottom baryon decays in the Bethe-Salpeter approach: Heavy to heavy semileptonic transitions, Phys. Rev. D **59**, 074016 (1999).
[60] H. W. Ke, X. H. Yuan, X. Q. Li, Z. T. Wei, and Y. X. Zhang, $\Sigma_b \to \Sigma_c$ and $\Omega_b \to \Omega_c$ weak decays in the light-front quark model, Phys. Rev. D **86**, 114005 (2012).
[61] W. Wang, F. S. Yu, and Z. X. Zhao, Weak decays of doubly heavy baryons: The $1/2 \to 1/2$ case, Eur. Phys. J. C **77**, 781 (2017).
[62] J. G. Korner and P. Kroll, Heavy quark symmetry at large recoil: The case of baryons, Z. Phys. C **57**, 383 (1993).
[63] N. Isgur and M. B. Wise, Heavy baryon weak form-factors, Nucl. Phys. **B348**, 276 (1991).
[64] H. Georgi, Comment on heavy baryon weak form-factors, Nucl. Phys. **B348**, 293 (1991).
[65] H. Y. Cheng and B. Tseng, 1/M corrections to baryonic form-factors in the quark model, Phys. Rev. D **53**, 1457 (1996); Erratum, Phys. Rev. D **55**, 1697(E) (1997).
[66] J. G. Korner, M. Kramer, and D. Pirjol, Heavy baryons, Prog. Part. Nucl. Phys. **33**, 787 (1994).
[67] H. W. Ke, N. Hao, and X. Q. Li, Revising $\Lambda_b \to \Lambda_c$ and $\Sigma_b \to \Sigma_c$ weak decays in the light-front quark model, Eur. Phys. J. C **79**, 540 (2019).
[68] H. Park *et al.* (HyperCP Collaboration), Evidence for the Decay $\Sigma^+ \to p\mu^+\mu^-$, Phys. Rev. Lett. **94**, 021801 (2005).
[69] V. Cirigliano, J. Jenkins, and M. Gonzalez-Alonso, Semileptonic decays of light quarks beyond the standard model, Nucl. Phys. **B830**, 95 (2010).
[70] T. Bhattacharya, V. Cirigliano, S. D. Cohen, A. Filipuzzi, M. Gonzalez-Alonso, M. L. Graesser, R. Gupta, and H. W. Lin, Probing novel scalar and tensor interactions from (ultra)cold neutrons to the LHC, Phys. Rev. D **85**, 054512 (2012).
[71] R. Dutta, A. Bhol, and A. K. Giri, Effective theory approach to new physics in $b \to u$ and $b \to c$ leptonic and semileptonic decays, Phys. Rev. D **88**, 114023 (2013).
[72] J. G. Korner and G. A. Schuler, Exclusive semileptonic heavy meson decays including lepton mass effects, Z. Phys. C **46**, 93 (1990).
[73] A. Kadeer, J. G. Korner, and U. Moosbrugger, Helicity analysis of semileptonic hyperon decays including lepton mass effects, Eur. Phys. J. C **59**, 27 (2009).
[74] T. Gutsche, M. A. Ivanov, J. G. Krner, V. E. Lyubovitskij, and P. Santorelli, Heavy-to-light semileptonic decays of Λ_b and Λ_c baryons in the covariant confined quark model, Phys. Rev. D **90**, 114033 (2014); Erratum, Phys. Rev. D **94**, 059902(E) (2016).
[75] T. Gutsche, M. A. Ivanov, J. G. Krner, V. E. Lyubovitskij, P. Santorelli, and N. Habyl, Semileptonic decay $\Lambda_b \to \Lambda_c + \tau^- + \bar{\nu}_\tau$ in the covariant confined quark model, Phys. Rev. D **91**, 074001 (2015); Erratum, Phys. Rev. D **91**, 119907(E) (2015).
[76] S. Shivashankara, W. Wu, and A. Datta, $\Lambda_b \to \Lambda_c \tau \bar{\nu}_\tau$ decay in the standard model and with new physics, Phys. Rev. D **91**, 115003 (2015).
[77] R. Dutta, Phenomenology of $\Xi_b \to \Xi_c \tau \nu$ decays, Phys. Rev. D **97**, 073004 (2018).
[78] M. Tanabashi *et al.* (Particle Data Group), Review of particle physics, Phys. Rev. D **98**, 030001 (2018).
[79] R. N. Faustov and V. O. Galkin (private communication).